# FIELD TESTING AND NUMERICAL MODELLING OF BRIDGE COLUMN TO CONTACT EXPLOSION

HRVOJE DRAGANIĆ, GORAN GAZIĆ, MARIO JELEČ & IVAN RADIĆ
Faculty of Civil Engineering and Architecture Osijek,
Josip Juraj Strossmayer University of Osijek, Croatia

ABSTRACT
Columns are among the most vulnerable elements of bridges due to their exposure to ongoing traffic beneath the bridge and the fact that their collapse often leads to the failure of the bridge superstructure. Contact explosions can compromise their integrity by damaging the concrete protective layer, weakening the core and severing reinforcing bars, ultimately leading to loss of stability. Such explosions may result from wartime efforts to sever critical transportation routes or controlled demolitions for infrastructure development. This study aims to evaluate the structural response of a bridge column subjected to a contact explosion through experimental testing and numerical modelling. A field test was conducted using a 1:3 scale column, designed based on an actual bridge column, with a spherical contact charge moulded from plastic explosive due to its chemical stability and handling properties. A steel support structure was implemented to replicate realistic end support conditions. The contact explosion caused concrete cratering and reinforcement bar bending but did not fully penetrate the column. Following experimental testing, a numerical simulation was conducted using Ansys Autodyn hydrocode software to replicate the field test. By varying erosion parameters, contact explosion damage was accurately simulated. Model validation was performed by comparing the experimentally measured damage area with the corresponding numerical results, ensuring consistency in size, shape, and deformation characteristics. The findings suggest that while significant localised damage occurs, the column retains partial structural integrity, highlighting the role of reinforcement in mitigating complete failure.
*Keywords: bridge column, collapse, contact charge, experimental testing, numerical modelling.*

## 1 INTRODUCTION

During the last decades, terrorist activities have emphasised the critical need for a better understanding of structural behaviour under both accidental and intentional blast loads. As key elements of transportation infrastructure, bridges are particularly vulnerable to explosion hazards. Bridge columns are crucial bridge components due to their exposure to ongoing traffic beneath the bridge and their vital role in supporting the superstructure, making their failure a direct threat to overall bridge stability.

The effect of blast loads on structures generally depends on whether the explosion is areal (distributed over a surface) or contact (occurring directly against a structure). Areal explosions typically induce a widespread structural response, whereas contact explosions cause localised damage, often resulting in cratering or full-thickness penetration of an element. The extent and nature of the damage are influenced by various factors, including the explosive's weight and shape, the thickness of the structural component, the ratio and arrangement of reinforcement bars, and the concrete grade used in reinforced concrete (RC) structures. In the case of RC bridge columns, contact explosions can severely compromise their integrity by damaging the protective concrete layer, weakening the core, and rupturing reinforcing bars, ultimately leading to structural instability. These explosions may occur during wartime efforts to disrupt key transportation routes or as controlled demolitions for infrastructure development.

Several studies experimentally investigated the contact explosions on RC elements (slabs [1]–[4], beams [5]–[7] or columns [8]–[13]), examining both un-retrofitted (plain) and

WIT Transactions on The Built Environment, Vol 215, © 2025 WIT Press
www.witpress.com, ISSN 1743-3509 (on-line)
doi:10.2495/SUSI250151

retrofitted elements. Most prior research focused on evaluating the efficacy of different retrofitting materials in enhancing the blast-resistance capabilities of such elements [14]–[16]. Previous studies classified the local damage modes into cratering, spalling, and breaching. However, the main damage modes of RC columns under close-in/contact explosion were also characterised by side cover concrete spalling, which has not been reported in relevant studies for RC slabs/walls. This phenomenon indicates that the propagation of stress waves is more complex and not one-dimensional in the cross-section of the column, which is significantly different from the one-dimensional propagation in the slab/wall elements.

Previous studies also highlight the complexity of understanding the damage modes of RC columns under contact explosion loads. Information on damage criteria or threshold curves remains scarce, and experimental research alone is prohibitively expensive [17]. Therefore, developing a reliable numerical model based on experimental data is essential for simulating damage modes and establishing a foundation for RC column design against contact explosions. Furthermore, measuring blast wave parameters in contact explosions is challenging, and the response of structural elements is not yet well understood. This has prompted a growing interest in numerical modelling to simulate such scenarios.

Numerical simulations are widely used to predict the response of RC structures to blast and impact loads, including concrete fracture and spalling. One common approach is the erosion model, which removes elements that meet predefined failure criteria, preventing excessive distortion of Lagrangian meshes. A review in Luccioni et al. [18] examines various erosion criteria and limits used to simulate concrete under blast loads, discussing their influence on damage predictions and their dependence on material properties, mesh size, and scaled distance. An alternative method, the Arbitrary Lagrangian–Eulerian (ALE)–FEM–smoothed particle hydrodynamics (SPH) coupling approach, unlike erosion models, preserves elements and has demonstrated strong agreement with experimental results [19], making it a promising technique for simulating concrete fragmentation under blast conditions. Several previous investigations conducted a numerical analysis of RC columns under contact explosion loads [20]–[22]. However, current numerical studies primarily focus on specific failure mechanisms, with models related to particular research objects, limiting their applicability to different cases and parameter analysis (even with minor variations in section size or shape). Some research conclusions remain unclear and require further validation [16]. Improving the accuracy of numerical models for RC columns under contact explosions and effectively verifying them against experimental data remain critical challenges.

RC bridge columns are critical structural elements, as their failure can lead to the collapse of the entire bridge. Evaluating their damage after an explosion is essential for assessing structural safety and collapse risk. This study investigates the response of a bridge column subjected to a contact explosion through experimental and numerical analyses. A field test was conducted on a 1:3 scale bridge column designed as an indented rectangular, as typically used in Croatian highways. A spherical plastic explosive charge generated the blast, while a steel support structure ensured realistic boundary conditions. The explosion caused concrete cratering and reinforcement bar deformation but did not fully penetrate the column. A high-fidelity numerical simulation was performed using Ansys Autodyn hydrocode software to analyse damage mechanisms further. Refining erosion parameters leads to the simulation more accurately replicating the observed damage, including the explosion-affected area's size, shape, and deformation. The results indicate that the column retains partial structural integrity while severe localised damage occurs, highlighting the reinforcement's crucial role in preventing catastrophic failure.

## 2 EXPERIMENTAL INVESTIGATION

The experiment's main objective is to evaluate the blast load resistance of the selected bridge column to contact explosion and provide a basis for validating and calibrating the developed numerical model.

### 2.1 Column geometry

The column geometry was selected based on a database containing the design documentation of all overpasses on Croatian roads and highways. A column with the most common geometry was selected and reproduced on a scale of 1:3. The scaling of the column was conducted concerning the theory of model similarity [23]. The scaled geometry of the selected column is presented in Fig. 1.

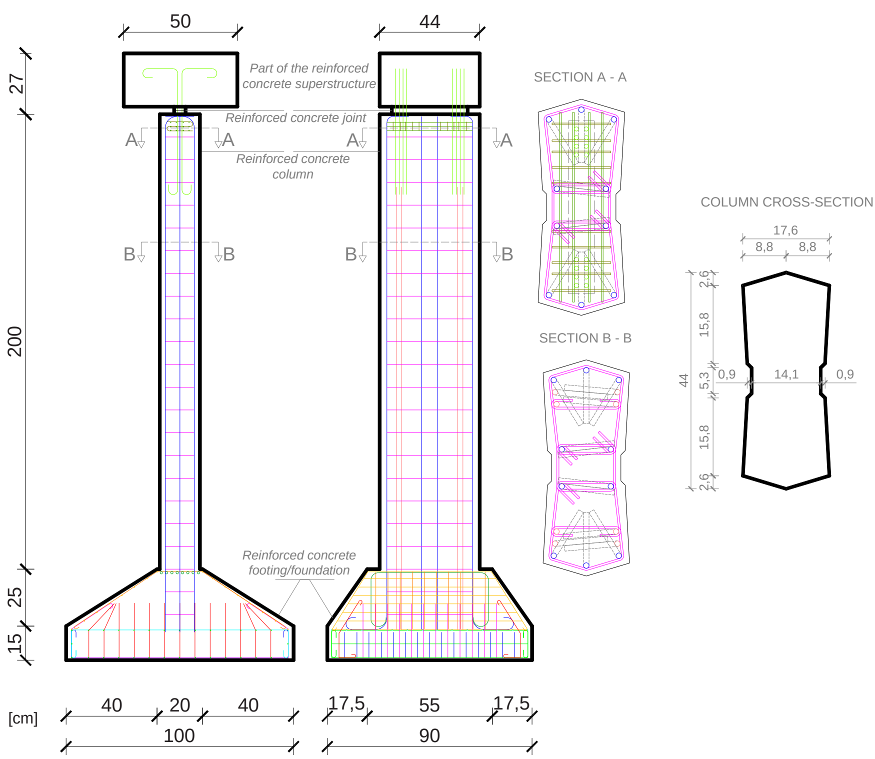


Figure 1: Tested column geometry.

### 2.2 Test setup

A steel reaction frame was designed to simulate real-life exploitation conditions. The reaction frame consisted of two parts, namely, a reinforced concrete foundation slab and a steel grid structure. The foundation slab was designed to accommodate and prevent horizontal displacements of the tested column footing. A steel grid structure consists of a part fixed to a foundation slab and an upper part designed as a lever. A fixed part provides boundary conditions of a column head beam and simulates the longitudinal stiffness of a bridge deck by preventing horizontal displacements and rotations. A lever part serves to introduce axial force into the column. The axial force was determined to simulate the weight of a bridge deck. A 250 g plastic explosive marked as PEP500 was used in the experiment. This type of plastic explosive is a mixture of 50% pentrite and 50% trinitrotoluene with a TNT equivalency of 1.3. The detonation was initiated using a lead-azide detonator capsule. The explosive was placed at a column surface at 40 cm from the column footing. The detonation capsule was placed horizontally, i.e. perpendicular to the column surface. The experiment was conducted in a corporation with the Croatian Army Forces. Fig. 2 shows the experimental test setup.

Figure 2: Test setup.

Free-field pressures were measured using pencil probes arranged in a semicircle during the test. Six pencil probes were used with a pressure capacity of 6895 kPa at temperatures from −73°C to +135°C, a resolution of 0.069 kPa/mV and a resonance frequency ≥ 400 kHz. Four probes were placed at 10 m and two at 2 m. All probes were placed at 1 m from the ground. The axial force was introduced by employing the Yale hydraulic press to the value of 130 kN. The axial force variation was measured by a force transducer having a capacity of 500 kN. The sensor disposition is presented in Fig. 3.

 
www.witpress.com, ISSN 1743-3509 (on-line)

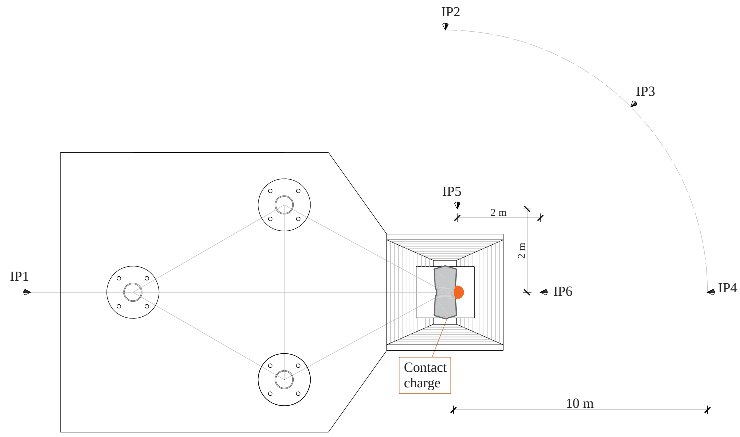


Figure 3: Sensor disposition.

## 2.3 Free-field pressure measurements

Obtained pressure–time history measurements are presented in Fig. 4(a) for pencil probes placed at 10 m and Fig. 4(b) for pencil probes placed at 2 m. The maximum free-field pressures are compared with the Kingery and Bulmash analytical predictions using eqns (1) and (2). The measured maximum pressures and analytical predictions are presented and compared in Tables 1 and 2.

$$U = K_0 + K_1 \times \log Z, \tag{1}$$

$$Y = 10^{(C_0 + C_1 \times U + C_2 \times U^2 + \cdots + C_N \times U^N)}, \tag{2}$$

where $Z$ is the scaled distance, $K$ and $C$ are constants and $Y$ is an incident or reflected pressure. The constants $K$ and $C$ change depending on the parameter $Y$.

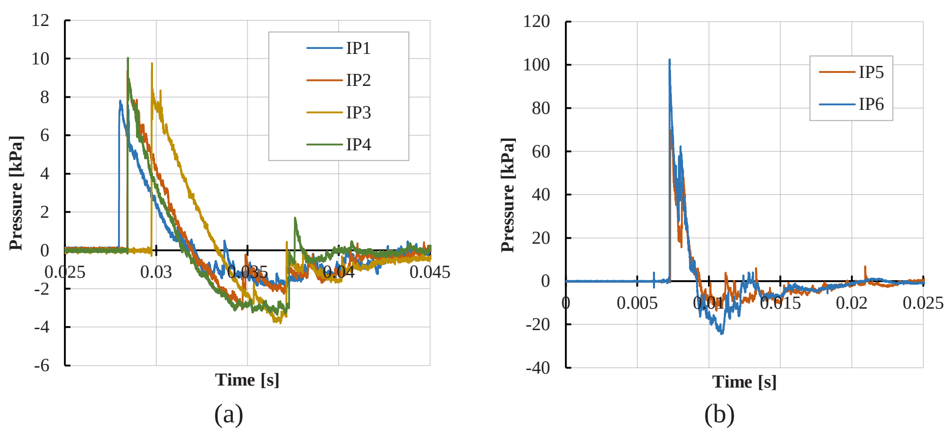


Figure 4: Free-field pressures at the distance of (a) 10 m; and (b) 2 m.

Table 1: Measured incident pressures (distance 10 m).

| **Range 10 m** | **IP1** | **IP2** | **IP3** | **IP4** | **Mean** | **St. dev.** | **Cov.** | **KB_IP** | **Rel. diff.** |
|---|---|---|---|---|---|---|---|---|---|
| Maximum (kPa) | 7.81 | 9.36 | 9.76 | 10.04 | 9.24 | 0.99 | 10.77 | 8.95 | 3.25 |
| Positive phase (ms) | 3.65 | 3.54 | 3.69 | 3.04 | 3.48 | 0.30 | 8.58 | 3.53 | 1.42 |

Table 2: Measured incident pressures (distance 2 m).

| **Range 2 m** | **IP5** | **IP6** | **Mean** | **St. dev.** | **Cov.** | **KB_IP** | **Rel. diff.** |
|---|---|---|---|---|---|---|---|
| Maximum (kPa) | 69.74 | 102.58 | 86.16 | 23.22 | 26.95 | 121.44 | 29.05 |
| Positive phase (ms) | 2.06 | 1.91 | 1.98 | 0.11 | 5.56 | 1.81 | 9.61 |

The Kingery and Bulmash analytical predictions agree with the measured values. The relative differences in the case of maximum free-field pressures measured at the distance of 10 m are negligible and equal to 3.25%. Somewhat higher, 29.05% relative differences are obtained for measurements at the distance of 2 m. Nevertheless, differences between measured and predicted positive phase duration are negligible for both measurement distances.

## 2.4 Damage description

Damage of the tested column is presented in Fig. 5. According to CSA-S850-12 [24], damage can be classified as hazardous failure. The observed damage is severe and localised around the explosive charge placement. The protective concrete cover was completely blown off from all sides of the column cross-section. Noticeable flying debris was found at a distance of up to 15 m. Columns' concrete core was reduced in the cross-sectional area due to spalling and fractured at a height of approximately 20 cm.

Figure 5: Damage to the tested column.

Nevertheless, a significant part of the column concrete core remained within, presumably due to rebar distance preventing dislodgement of the concrete. It is assumed that the dense layout of reinforcement bars caused a confinement effect, constraining the concrete core and preventing total perforation of the column. This assumption can be justified because the axial force reduction was negligible; an approximate loss of 10% was observed, as presented in Fig. 6.

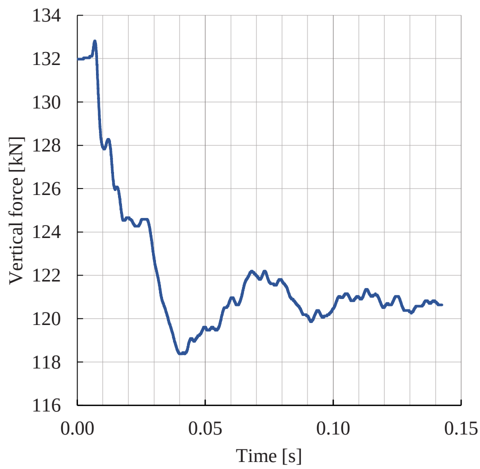


Figure 6: Axial force variation through time.

## 3 NUMERICAL MODELLING

### 3.1 Modelling approach

Contact explosion was modelled using Ansys Autodyn hydrocode software [25] specialised for simulating fluid–structure interaction. As Section 2 described, the column was supported by a steel support structure simulating fixed boundary conditions at the column head. The numerical model was simplified by directly implementing fixed boundary conditions to the column head, omitting the steel support structure numerical model. Further simplification was implemented by using symmetry. Only one-half of the column was modelled with a symmetry plane positioned in the column's longitudinal axis. The concrete part of the column was modelled as a solid element, while reinforcement was modelled as a beam element connected with a contact element, enabling their mutual deformation. Fig. 7 shows the column numerical model in Ansys Autodyn with details regarding boundary conditions and element types.

### 3.2 Material models

Concrete behaviour was modelled using the RHT material model [26]. The RHT (Riedel–Hiermaier–Thoma) concrete material model is widely used in numerical simulations to describe the dynamic behaviour of concrete under high strain rates and complex loading conditions, such as impacts and explosions. It incorporates pressure-dependent strength, strain rate effects, damage accumulation, and failure criteria. Due to its ability to capture

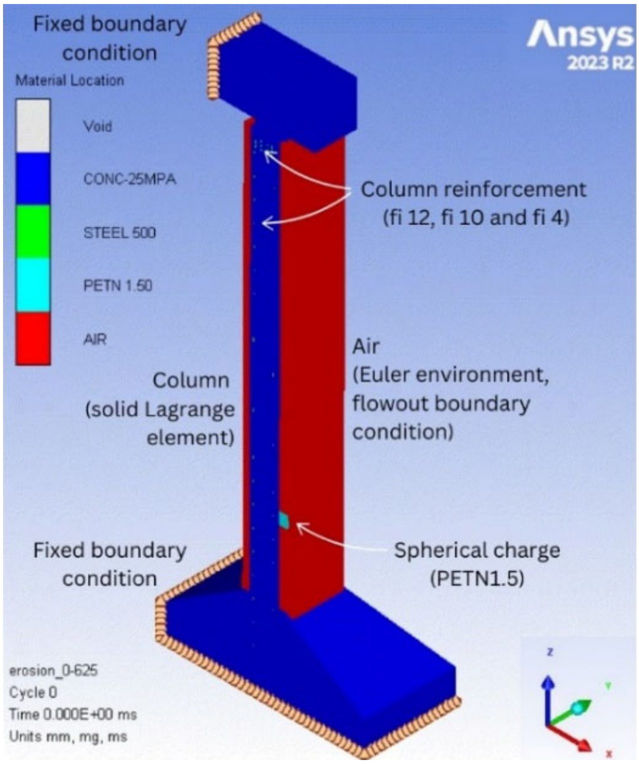


Figure 7: Contact explosion numerical model.

nonlinear stress–strain responses, progressive damage, and brittle failure modes, the RHT model is particularly suitable for simulating protective structures, impact analyses, and blast-resistant design scenarios.

Reinforcement material was modelled using the Johnson–Cook material model [27]. The Johnson–Cook (J–C) steel material model is commonly employed for simulating the behaviour of metals, particularly steel, under large strains, high strain rates, and elevated temperatures. It captures strain hardening, strain rate sensitivity, and thermal softening effects, making it especially suitable for impact, penetration, machining, and crash analyses. Due to its simplicity and robustness, the J–C model is widely used in explicit finite element analyses of dynamic problems involving metals.

The explosive was modelled as a spherical charge using the PETN1.5 material model. It incorporates the Jones–Wilkins–Lee (JWL) [28] equation of state to represent the explosive's pressure–volume–energy relationship during detonation. Due to its accuracy in capturing detonation pressure, energy release, and expansion of explosive products, PETN1.5 is particularly suitable for modelling high-explosive charges in structural response analyses, impact simulations, and blast-resistant design.

Column and charge were placed into an air environment modelled as an ideal gas [29]. The air material model as an ideal gas represents air behaviour based on the ideal gas equation of state, relating pressure, volume, and temperature through simple thermodynamic relations. It is commonly used in numerical simulations involving aerodynamic flows, blast wave propagation, shock interactions, and fluid–structure interaction problems. Due to its simplicity, computational efficiency, and reasonable accuracy for most engineering scenarios involving low to moderate pressures and temperatures, the ideal gas model for air is widely employed in structural, aerodynamic, and blast analyses.

### 3.3 Model verification

One of the parameters governing the damage behaviour activated was erosion. The geometric strain erosion parameter (instantaneous) defines a numerical erosion criterion used in explicit finite element simulations to remove excessively distorted elements once they reach a specified strain threshold. This parameter helps maintain numerical stability and computational efficiency by preventing unrealistic deformation and element inversion, which is particularly useful in high-strain scenarios such as impacts, penetration and blast simulations.

The default value of the erosion parameter is set at 0.5. The numerical study incorporated variations of erosion parameters to validate the model against experimental data. Erosion was varied in a step of 0.125 considering the following values: 0.375, 0.5, 0.625, 0.75, 0.875 and 1.0. For each erosion value, the figure of simulated damage is given in Tables 3 and 4. The most suitable erosion value was identified based on the visual comparison and damage area analysis. Calculated relative differences between the experimental and numerical values are given in Table 5.

## 4 DISCUSSION

Based on a comparison between the damaged areas observed in numerical simulations and those recorded during experimental field tests, it can be concluded that the most accurate correlation is achieved when a geometric strain erosion criterion of 0.5 is applied in the simulation (Tables 3, 4 and 5). This value corresponds to the default value provided by the RHT material model. Further analysis of the column's cross-sectional damage reveals that the numerical model predicts more extensive concrete damage than observed in the field.

Table 3: Column damage based on erosion criterion variation (views at 2 ms).

| Column damage | | Geometric strain erosion criterion | | | | | |
|---|---|---|---|---|---|---|---|
| | | 0.375 | 0.500 | 0.625 | 0.750 | 0.875 | 1.000 |
| Front face | 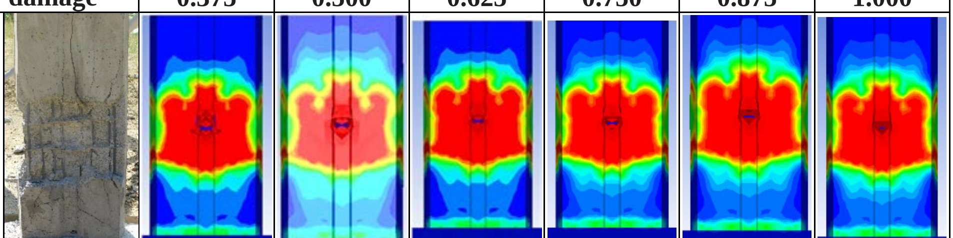 | | | | | | |
| Back face | 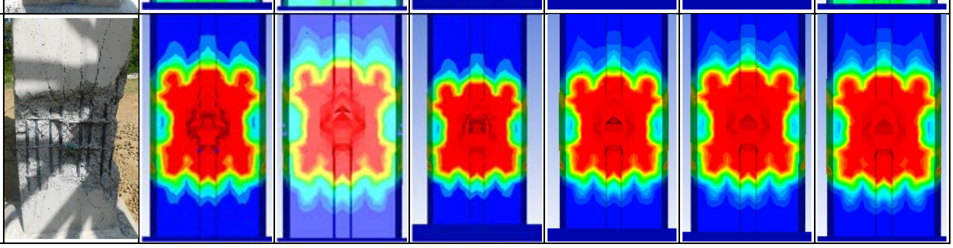 | | | | | | |

Table 4: Column damage based on erosion criteria variation (cross-section at 2 ms).

| Column damage | | Geometric strain erosion criterion | | | | | |
|---|---|---|---|---|---|---|---|
| | | 0.375 | 0.500 | 0.625 | 0.750 | 0.875 | 1.000 |
| Front face |  | 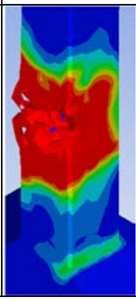 | 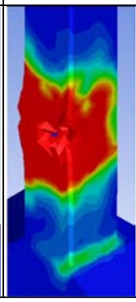 | 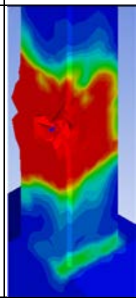 | 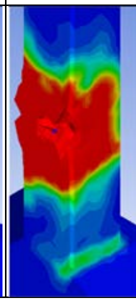 | 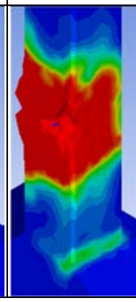 | 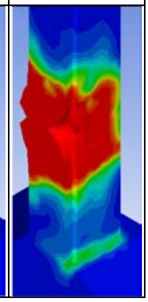 |

Table 5: Damage area for field test and numerical simulations.

| Erosion | Front | Exp | RD (%) | Back | Exp | RD (%) |
|---|---|---|---|---|---|---|
| 0.375 | 1550 | 1499 | 3.4 | 1885 | 2233 | 15.6 |
| 0.500 | 1507 | 1499 | 0.5 | 1940 | 2233 | 13.1 |
| 0.625 | 1558 | 1499 | 3.9 | 1889 | 2233 | 15.4 |
| 0.750 | 1562 | 1499 | 4.2 | 1694 | 2233 | 24.1 |
| 0.875 | 1660 | 1499 | 10.7 | 1768 | 2233 | 20.8 |
| 1.000 | 1634 | 1499 | 9.0 | 1828 | 2233 | 18.1 |

RD, relative difference.

Table 4 shows that the explosive charge used in the experimental test did not fully perforate the column. However, a significant portion of the reinforced concrete cover was removed near the detonation point. A thin layer of concrete from the core remained intact within the reinforcement ‘cage’, suggesting that while surface damage was severe, the inner core retained some structural integrity.

In contrast, the numerical simulation produced a damage pattern visually similar to the experimental results using the geometric strain erosion criterion. However, a closer examination of the simulated column cross-section indicates that the blast wave penetrates deeper into the structure, suggesting localised perforation at the point of charge contact. The simulation predicts a concentrated zone of damage around the detonation point, yet the erosion of elements is limited and highly localised, regardless of the erosion threshold applied. This discrepancy between visual surface damage and internal material erosion in the simulation is highlighted in Tables 3 and 4, which show that while damage is concentrated near the charge, the elements in the simulation are not entirely eroded beyond this localised area. The damage area trend based on applied erosion value can be seen in Fig. 8.

## 5 CONCLUSION

The field test results and corresponding numerical analyses demonstrate that bridge columns subjected to contact explosions can sustain severe localised damage but retain partial structural integrity. In the experimental investigation, a 1:3 scale column incurred significant cratering and spalling around the charge placement, with complete loss of concrete cover and core fracturing; however, the dense reinforcement layout helped to confine the concrete and prevent complete perforation. Measured free-field pressures agreed well with the Kingery and Bulmash analytical predictions, further validating the experimental methodology.

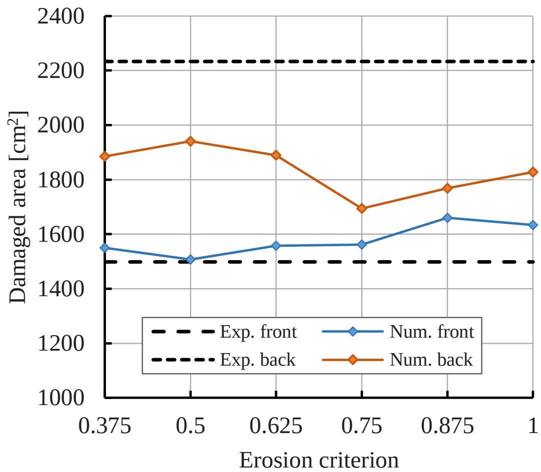


Figure 8: Damaged area for field test and numerical simulations.

In the numerical study, simulations using the RHT material model for concrete and the J–C model for steel reinforcement effectively replicated many aspects of the observed damage. A geometric strain erosion criterion of 0.5 yielded the best correlation between experimental and numerical results, capturing the extent of localised damage and the remaining core integrity. Nonetheless, the simulation predicted a slightly deeper penetration of the blast wave than the physical specimen, highlighting the need for continued refinement of numerical parameters and material modelling approaches.

Overall, the findings underscore the critical influence of reinforcement in mitigating catastrophic failure from contact explosions and confirm that properly calibrated numerical models can be valuable tools for assessing blast resistance. The ability of the column to maintain partial load-bearing capacity despite major local damage emphasises the importance of robust detailing and accurate computational methods when designing and evaluating bridge columns for blast resistance.

## ACKNOWLEDGEMENTS

The research presented in this paper has been partly supported by the Croatian Science Foundation (HRZZ) under the project UIP-2017-05-7041 ‘Blast Load Capacity of Highway Bridge Columns’, and support for this research is gratefully acknowledged. The authors would like to thank all individuals who provided help during the research.

## REFERENCES

[1] Dua, A. & Braimah, A., Assessment of reinforced concrete slab response to contact explosion effects. *Journal of Performance of Constructed Facilities*, **34**(4), 04020061, 2020.

[2] Wang, W. et al., Study on antiexplosion performance of reinforced concrete slabs strengthened with POZD coated steel plate under contact explosion. *Engineering Failure Analysis*, **140**, 106589, 2022.

[3] Yang, G. et al., Experimental and numerical study of damage characteristics of RC slabs subjected to air and underwater contact explosions. *Marine Structures*, **66**, pp. 242–257, 2019.

[4] Cai, R. et al., Size effect on reinforced concrete slabs under direct contact explosion. *Engineering Structures*, **252**, 113656, 2022.
[5] Zhu, W. et al., Blast resistant performance and damage mechanism of steel reinforced concrete beams under contact explosion. *Engineering Structures*, **315**, 118472, 2024.
[6] Yang, C. et al., Damage of full-scale reinforced concrete beams under contact explosion. *International Journal of Impact Engineering*, **163**, 104180, 2022.
[7] Jun-Hua, H. et al., Dynamic response and damage assessment of a prestressed T-shaped simply supported girder bridge under contact explosion. *Structures*, **48**, pp. 40–52, 2023.
[8] Williamson, E.B., Blast-resistant highway bridges: Design and detailing guidelines. *Transportation Research Board*, **645**, 2010.
[9] Wu, K.-C., Li, B. & Tsai, K.-C., The effects of explosive mass ratio on residual compressive capacity of contact blast damaged composite columns. *Journal of Constructional Steel Research*, **67**(4), pp. 602–612, 2011.
[10] Fujikake, K. & Aemlaor, P., Damage of reinforced concrete columns under demolition blasting. *Engineering Structures*, **55**, pp. 116–125, 2013.
[11] Roller, C. et al., Residual load capacity of exposed and hardened concrete columns under explosion loads. *Engineering Structures*, **55**, pp. 66–72, 2013.
[12] Yuan, S. et al., A study of RC bridge columns under contact explosion. *International Journal of Impact Engineering*, **109**, pp. 378–390, 2017.
[13] Li, M. et al., Experimental and numerical study on damage mechanism of CFDST bridge columns subjected to contact explosion. *Engineering Structures*, **159**, pp. 265–276, 2018.
[14] Draganić, H., Gazić, G. & Varevac, D., Experimental investigation of design and retrofit methods for blast load mitigation: A state-of-the-art review. *Engineering Structures*, **190**, pp. 189–209, 2019.
[15] Lukić, S. & Draganić, H., Blast loaded columns: State of the art review. *Applied Sciences*, **11**, 2021. https://doi.org/10.3390/app11177980.
[16] Yuan, S. et al., A review on close-in blast performance of RC bridge columns. *Journal of Traffic and Transportation Engineering (English Edition)*, **10**(4), pp. 675–696, 2023.
[17] Zhang, C., Gholipour, G. & Mousavi, A.A., Blast loads induced responses of RC structural members: State-of-the-art review. *Composites Part B: Engineering*, **195**, 108066, 2020.
[18] Luccioni, B.M., Aráoz, G.F. & Labanda, N.A., Defining erosion limit for concrete. *International Journal of Protective Structures*, **4**(3), pp. 315–340, 2013.
[19] Wang, Z. et al., Numerical prediction of blast fragmentation of reinforced concrete slab using ALE–FEM–SPH coupling method. *Finite Elements in Analysis and Design*, **220**, 103948, 2023.
[20] Xiao, Y. et al., Concrete spalling behavior and damage evaluation of concrete members with different cross-sectional properties under contact explosion. *International Journal of Impact Engineering*, **181**, 104753, 2023.
[21] Mejía, N. et al., Damage assessment of RC columns under the combined effects of contact explosion and axial loads by experimental and numerical investigations. *Engineering Structures*, **254**, 113776, 2022.
[22] Liu, L. et al., Experimental and numerical study of CFRP protective RC piers under contact explosion. *Composite Structures*, **234**, 111658, 2020.
[23] Harris, H. & Sabnis, G.M., *Structural Modeling and Experimental Techniques*, 2nd ed., CRC Press, 1999.

[24] CSA Group, S850-12 Design and Assessment of Buildings Subjected to Blast Loads. Mississauga, 2012.

[25] Ansys Autodyn, *Theory Manual Revision 4.3*, Century Dynamics: Concord, CA, USA, 2005.

[26] Thoma, K., Riedel, W. & Hiermaier, S., Mesomechanical modeling of concrete shock response experiments and linking to macromechanics by numerical analysis. *Proceedings of European Conference on Computational Mechanics*, 1999.

[27] Johnson, G.R. & Cook, W.H., Fracture characteristics of three metals subjected to various strains, strain rates, temperatures and pressures. *Engineering Fracture Mechanics*, **21**(1), pp. 31–48, 1985.

[28] Lee, E., Hornig, H. & Kury, J., Adiabatic expansion of high explosive detonation products. University of California Radiation Laboratory at Livermore, Livermore, CA, USA, 1968.

[29] Rogers, G.F.C. & Mayhew, Y.R., *Thermodynamic and Transport Properties of Fluids*, John Wiley and Sons, 1995.